RNA Biology 10:8, 1233–1239; August 2013; © 2013 Landes Bioscience

Profiles of piRNA abundances at emerging or established piRNA loci are determined by local DNA sequences

Augustin de Vanssay[1,†], Anne-Laure Bougé[2,‡], Antoine Boivin[1], Catherine Hermant[1], Laure Teysset[1], Valérie Delmarre[1], Stéphane Ronsseray[1,*], and Christophe Antoniewski[2,*]

[1]Epigenetic Repression and Transposable Elements; Laboratoire Biologie du Développement; UMR7622; CNRS-Université Pierre et Marie Curie; Paris, France; [2]Drosophila Genetics and Epigenetics; Laboratoire Biologie du Développement; UMR7622; CNRS-Université Pierre et Marie Curie; Paris, France

Current affiliation: [†]Institut Jacques Monod; CNRS; UMR 7592; Université Diderot; Sorbonne Paris Cité; Paris, France; [‡]Drosophila Normal and Pathological Neurobiology; INSERM U661 - Institut de Génomique Fonctionnelle; Montpellier, France

Piwi-interacting RNAs (piRNAs) ensure transposable element silencing in *Drosophila*, thereby preserving genome integrity across generations. Primary piRNAs arise from the processing of long RNA transcripts produced in the germ line by a limited number of telomeric and pericentromeric loci. Primary piRNAs bound to the Argonaute protein Aubergine then drive the production of secondary piRNAs through the "ping-pong" amplification mechanism that involves an interplay with piRNAs bound to the Argonaute protein Argonaute-3. We recently discovered that clusters of P-element-derived transgenes produce piRNAs and mediate silencing of homologous target transgenes in the female germ line. We also demonstrated that some clusters are able to convert other homologous inactive transgene clusters into piRNA-producing loci, which then transmit their acquired silencing capacity over generations. This paramutation phenomenon is mediated by maternal inheritance of piRNAs homologous to the transgenes. Here we further mined our piRNA sequencing data sets generated from various strains carrying transgenes with partial sequence homology at distinct genomic sites. This analysis revealed that same sequences in different genomic contexts generate highly similar profiles of piRNA abundances. The strong tendency of piRNAs for bearing a U at their 5' end has long been recognized. Our observations support the notion that, in addition, the relative frequencies of Drosophila piRNAs are locally determined by the DNA sequence of piRNA loci.

Keywords: *Drosophila melanogaster*, piRNA biogenesis, germline, epigenetics, paramutation, transposable elements, argonaute proteins

Submitted: 06/08/2013

Accepted: 07/15/2013

http://dx.doi.org/10.4161/rna.25756

*Correspondence to: Stéphane Ronsseray, Email: stephane.ronsseray@upmc.fr; Christophe Antoniewski; Email: christophe.antoniewski@upmc.fr

Repression of Transposable Elements (TEs) in the *Drosophila* germline by Piwi-interacting RNAs (piRNAs) preserves genome integrity and prevents the transmission to next generations of mutations induced by TE mobilization. Over the past years, major progresses have been made in the understanding of the mechanisms of piRNA biogenesis and activity in flies.[1]

The *Drosophila melanogaster* genome carries a limited number of loci (~140) that contain arrays of TE fragments and are most often bi-directionally transcribed in the germ cells to produce both sense and antisense piRNA precursor transcripts. In contrast, a single *flamenco* TE cluster is uni-directionally transcribed in the ovarian follicle cells surrounding the germ cells, produces antisense piRNA precursors exclusively, and is mainly involved in silencing of a specific class of retrotransposons called *errantiviruses*. piRNA precursor transcripts in the germ cells reach the nuage, a diffuse structure surrounding the nucleus where a number of components from the piRNA pathway accumulate.[2] In the nuage, the cleavage of piRNA precursor transcripts by the nuclease Zucchini and subsequent 3' shortening give rise to primary 23–28-nt long piRNAs.[3,4] Antisense primary piRNAs bound to the PIWI Argonaute

Aubergine (Aub) can then enter the so-called "ping-pong" amplification step by pairing with sense piRNA precursors. This results in the slicing of precursors and generates secondary sense piRNAs, which, in turn, associate with the PIWI Argonaute AGO3 and guide the cleavage of more antisense precursors.[5,6] Thus, the ping-pong mechanism drives the amplification of a population of antisense piRNAs that overlap by 10 nt with sense piRNAs. Indeed, this 10 nt overlap "signature" reflects the piRNA-guided cleavage of piRNA precursors by PIWI Argonautes, which occurs between nucleotide 10 and 11, relative to the 5' end of the guide piRNA. As another feature of primary piRNAs is their bias for having a 5' uridine (1U), which is probably due to the nucleotide preferences of Aubergine and Piwi proteins, the ping-pong mechanism amplifies of population of AGO3-associated secondary piRNAs with a bias for an adenine at position 10 (10A).

Although the ping-pong amplification provides an obvious mechanism of TE transcript degradation, TE silencing by Piwi-bound piRNAs may also operate at transcriptional level (TGS). The Piwi Argonaute protein distributes in both cytoplasm and nucleus.[6,7] In ovarian follicle cells, which are devoid of Aub and AGO3, the slicer activity of Piwi protein is not required for TE silencing, whereas a mutation impairing Piwi nuclear localization abolishes TE silencing.[8,9] Moreover, in a follicle-derived cell line, Piwi-bound piRNAs target TE sequences dispersed in euchromatin, reduce their Pol II occupancy, and trigger the formation of H3K9me3 repressive marks.[10] A recent study suggests that Piwi may similarly mediate TGS in some somatic adult tissues.[11]

In contrast to the progresses made on the biogenesis and silencing mechanisms by piRNAs, what defines piRNA-producing loci and how the production of piRNAs by these loci is regulated is not well understood. It is likely that the repetitive nature of piRNA loci is an important *cis*-regulatory feature for the production of primary piRNAs. Besides, the deposition of H3K9me3 mark at TE clusters by dSETDB1 was involved in piRNA production[12] and the HP1-family protein Rhino binds to dual strand clusters to promote their transcription and piRNA production.[13] However, the mechanisms by which these factors are targeted to piRNA loci are still unknown.

Our recent finding that piRNAs are vectors of a paramutation in *Drosophila*[14] adds another layer of complexity by indicating that maternally deposited piRNAs can trigger *trans*-generational emergence of some piRNA-producing loci. In previous studies, we had shown that two *P{lArB}* transgenes inserted in Telomeric Associated Sequences (TAS) and containing the *Adh* and *rosy* genes of *D. melanogaster* and a bacterial *lacZ* gene, repress germline expression of *lacZ* reporter transgenes inserted at a distance, through a homology-dependent silencing mechanism called *Trans*-Silencing Effect (TSE).[15,16] These telomeric *P{lArB}* insertions (hereafter referred to as *P-1152*) mimic natural *P*-elements whose insertions in TAS results in the production of *P-element*-derived piRNAs and establishment of maternally transmitted *P*-element repression.[17-19] In addition to *P-1152*, we found that *T-1*, a repeat cluster of 7 *P{lacW}* transgenes containing the *white* and *lacZ* genes and inserted in the middle of chromosome arm 2R,[20] also produces piRNAs and triggers strong TSE.[21] In contrast, other *P{lacW}* clusters inserted at the exact same location, including *BX2* that has the same number of *P{lacW}* repeats as *T-1*, did not induce detectable TSE. TSE strongly correlates with piRNA production, as small RNA sequencing from *P-1152* or *T-1* but not from *BX2* ovaries revealed numerous transgene-derived piRNAs. Strikingly, when *BX2* males were crossed with *T-1* females (**Fig. 1A**), the female progeny containing the *BX2* chromosome acquired strong TSE capacity (noted as *BX2**). This effect was observed without *T-1* chromosome inheritance from the *T-1* mother and was then stably inherited over generations. Moreover, when *BX2** females were crossed with *BX2* males (**Fig. 1B**), the female progeny containing the "naïve" *BX2* chromosome in turn acquired strong TSE capacity (noted as *BX2*²*). Thus, the *BX2* to *BX2** transition is a paramutation, previously defined as an epigenetic interaction between two alleles of a locus, through which one allele induces a heritable modification of the other allele without modifying the DNA sequence.[22,23] Moreover, the acquired and stable TSE capacities of the *BX2** and *BX2*²* lines correlated with the production of a high level of *BX2*-derived piRNAs in ovaries, and were abolished in *aubergine* but not in *Dicer-2* mutants. Altogether, these results imply that piRNAs can play the role of a maternally deposited signal that first triggers and then maintains over generations the production of piRNA from a previously inactive locus (**Fig. 1**). Interestingly, a recent work suggests that resembling mechanisms may account for the acquisition of *I-element* repression capacity in *Drosophila* strains devoid of functional copies of this LINE-like element.[24]

Our small RNA sequencing of small RNA libraries[14] prepared using an Illumina set of RNA adaptor (*Illum*) revealed that piRNA abundance profiles from *T-1* and *BX2** ovaries after two generations (G2) are quite similar. This similarity is apparent from the observed degree of symmetry when either sense (**Fig. 2A**) or antisense (**Fig. 2B**). $T\text{-}1_{Illum}$ and $BX2^{*}G2_{Illum}$ piRNA abundances were plotted on the same maps. Accordingly, abundances of sense as well as antisense piRNAs from $T\text{-}1_{Illum}$ and $BX2^{*}G2_{Illum}$ showed a strong correlation (**Fig. 2C and D**). Note that although the Spearman correlation coefficient (based on ranking correlation) is less impressive in these analyses, it is more appropriate and robust than the Pearson correlation coefficient (based on linear regression of the values) when the data do not necessarily come from a bivariate normal distribution, which is likely the case for piRNA abundance variables. Cloning biases impact the small RNA libraries generated,[25] thereby altering quantitation and possibly accounting for the strong correlations between the $T\text{-}1_{Illum}$ and $BX2^{*}G2_{Illum}$ profiles of piRNA abundances. Indeed, these cloning biases were reflected by the lower correlations between the sense and antisense $BX2^{*}G2_{Illum}$ profiles and the sense and antisense $BX2^{*}G2_{IdT}$ profiles obtained under the same genetic settings but using another *IdT* set of RNA adapters (**Table 1**, Pearson cor. 0.38 and 0.26,

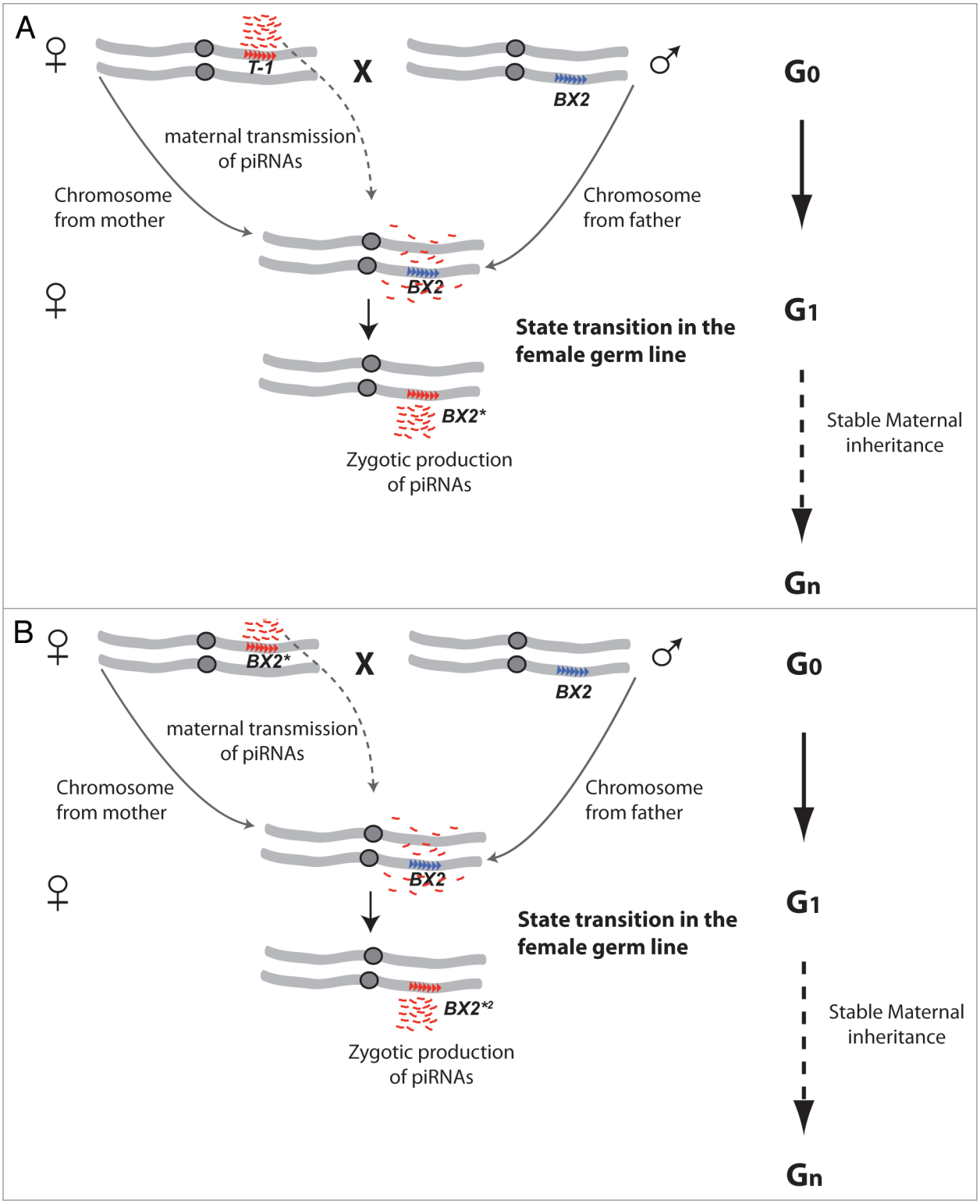

Figure 1. Paramutation of the *BX2* locus involves maternally inherited *T-1* piRNAs. (**A**) Whereas the *T-1* transgene cluster produces piRNAs (small red dashes), the *BX2* transgene cluster does not; these distinct properties are completely stable over generations. When *T-1* females are crossed to *BX2* males (G0), the female progeny (G1) that inherited the *BX2* chromosome from fathers and *T-1*-derived piRNAs from the mother (but not the *T-1* chromosome) start to zygotically produce high levels of *BX2*-derived piRNAs. The inactive (blue) to active (red) state transition of the *BX2* locus is noted with an asterisk (*BX2**). This so-called paramutation can be further maternally inherited in the next generations (Gn). (**B**) Similarly as in (**A**), maternal inheritance of *BX2**-derived piRNAs triggers the state transition of an inactive *BX2* loci in G1, associated to zygotic production of piRNAs. This second-order paramutation is noted as *BX2*^{*2}* and can be further maternally inherited in the next generations (Gn). The seven repeats of the *P{lacW}* transgene in the *T-1* and *BX2* loci are represented by blue or red arrowheads, depending on the states of the loci (active in red, inactive in blue).

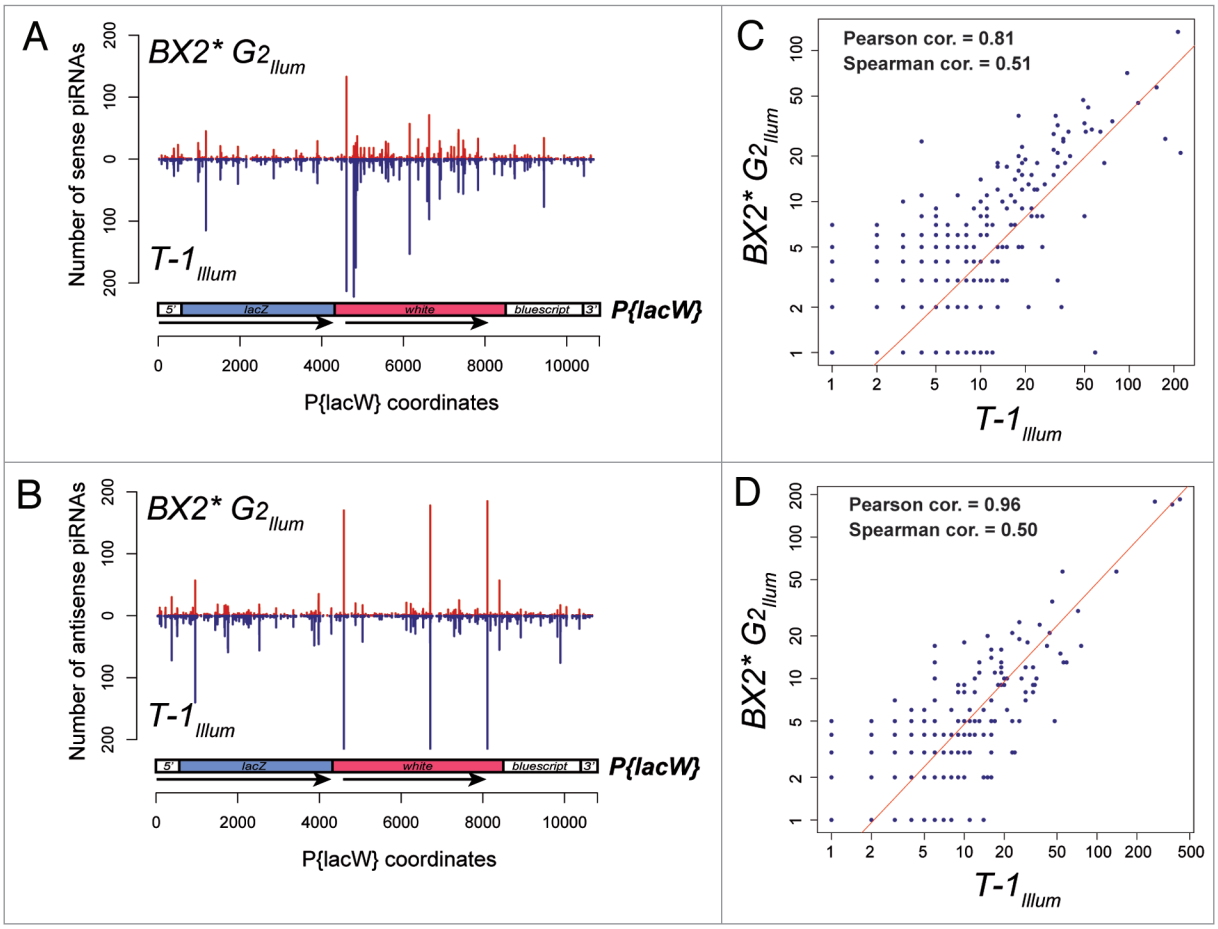

Figure 2. The profiles of piRNA abundances in *T-1* and *BX2** ovaries show strong correlations. The numbers of piRNAs (23–28 nt small RNA reads) matching the sense strand (**A**) or the antisense strand (**B**) of *P{lacW}* in *T-1* (blue bars) or *BX2** ovaries (red bars) were plotted relatively to the *P{lacW}* nucleotide coordinates. Number of reads of individual sense (**C**) or antisense (**D**) piRNA sequences matching *P{lacW}* in *T-1* (x-axes) or *BX2** (y-axes) ovaries were plotted in scatter plots. The *Illum* index indicates that the small RNA libraries were prepared using the same Illumina set of RNA adapters (see ref. 14). The red line corresponds to the linear regression of the data. The Pearson and Spearman correlation coefficients were computed using the cor.test function in R and the methods "pearson" or "spearman."

Spearman cor. 0.28 and 0.27). However, these correlations were still highly significant (*P* values < 2.2e–16 in both Pearson and Spearman correlation tests). In addition, sense and antisense profiles from $BX2^*G2_{IdT}$ and $T\text{-}1_{Illum}$ obtained using different set of RNA adapters during library preparations remain also significantly correlated (**Table 1**, Pearson cor. 0.28 and 0.27, Spearman cor. 0.29 and 0.27, all *P* values < 2.2e–16). In agreement with a previous report,[26] these data suggest that cloning biases in small RNA libraries are not sufficient to explain correlations between profiles of piRNA abundances and that these profiles are in part determined by the DNA sequence of piRNA-producing loci. The analysis of small RNA libraries all prepared using the same IdT set of RNA adapters further supports this conclusion, as both sense and antisense piRNA abundance profiles remain strongly correlated in the *BX2** line after 42 generations (**Table 1**, $BX2^*G2_{IdT}$ vs. $BX2^*G42_{IdT}$) as well as in a $BX2^{*2}$ line after 36 generations (**Table 1**, $BX2^*G2_{IdT}$ vs. $BX2^{*2}G36_{IdT}$).

Interestingly, the *P{lArB}* transgenes of the telomeric *P-1152* locus and the *P{lacW}* transgenes at the *BX2* and *T-1* loci in the middle of chromosome *2R* have some DNA sequences in common, as evidenced by a dot matrix view of a Blast alignment of the two types of transgenes (**Fig. 3A**). Namely, *P{lArB}* and *P{lacW}* share the *lacZ* gene fused to the 3' UTR of *hsp70* as well as a common pBluescript-derived backbone either in direct or in inverse orientation relatively to *lacZ* (**Fig. 3**). In contrast, the *Adh* coding sequences fused to a 620 bp DNA fragment of unknown origin and the *rosy* marker gene are specific to *P{lArB}* whereas the *white* marker gene is specific to *P{lacW}*. This situation of two piRNA-producing loci located at distinct genomic positions but sharing partial homology allowed us to test whether DNA sequences locally impact the profiles of piRNA abundances. To this aim, we computed the Spearman correlations between all possible 500 nt profile segments generated by the sense strand of *P{lArB}* in *P-1152* ovaries and all possible 500 nt profile segments generated by both sense and antisense strands of *P{lacW}* in *T-1* ovaries (**Fig. 3B**, two times ~181 millions of correlations were computed). We repeated the same procedure with all possible 500 nt profile segments generated by

Table 1. Pearson and Spearman correlation coefficients of *BX2** and *T-1* profiles of piRNA abundances

Pearson	s BX2*G2$_{IdT}$	as BX2*G2$_{IdT}$	s BX2*G42$_{IdT}$	as BX2*G42$_{IdT}$	s BX2*^{2}G36$_{IdT}$	as BX2*^{2}G36$_{IdT}$	s BX2*G2$_{Illum}$	as BX2*G2$_{Illum}$	s T-1$_{Illum}$	as T-1$_{Illum}$
s BX2*G2$_{IdT}$	*1*	−0.01	**0.88**	−0.01	**0.91**	−0.01	**0.38**	−0.01	**0.28**	−0.01
as BX2*G2$_{IdT}$		*1*	−0.01	**0.89**	−0.01	**0.88**	−0.01	**0.26**	0.00	**0.27**
s BX2*G42$_{IdT}$			*1*	−0.01	**0.91**	−0.01	**0.28**	−0.01	**0.22**	−0.01
as BX2*G42$_{IdT}$				*1*	−0.01	**0.88**	−0.01	**0.17**	0.00	**0.18**
s BX2*^{2}G36$_{IdT}$					*1*	−0.02	**0.29**	−0.01	**0.22**	−0.01
as BX2*^{2}G36$_{IdT}$						*1*	−0.01	**0.20**	−0.01	**0.21**
s BX2*G2$_{Illum}$							*1*	−0.01	**0.81**	−0.01
as BX2*G2$_{Illum}$								*1*	0.00	**0.96**
s T-1$_{Illum}$									*1*	*0*
as T-1$_{Illum}$										*1*
			IdT adaptor set					**Illumina adaptor set**		

Spearman	s BX2*G2$_{IdT}$	as BX2*G2$_{IdT}$	s BX2*G42$_{IdT}$	as BX2*G42$_{IdT}$	s BX2*^{2}G36$_{IdT}$	as BX2*^{2}G36$_{IdT}$	s BX2*G2$_{Illum}$	as BX2*G2$_{Illum}$	s T-1$_{Illum}$	as T-1$_{Illum}$
s BX2*G2$_{IdT}$	*1*	−0.04	**0.55**	−0.03	**0.57**	−0.03	**0.28**	−0.01	***0.29***	−0.02
as BX2*G2$_{IdT}$		*1*	−0.04	**0.46**	−0.05	**0.50**	−0.02	**0.27**	−0.03	***0.27***
s BX2*G42$_{IdT}$			*1*	−0.04	**0.58**	−0.04	**0.30**	−0.01	**0.31**	−0.02
as BX2*G42$_{IdT}$				*1*	−0.04	**0.51**	−0.02	**0.27**	−0.03	**0.29**
s BX2*^{2}G36$_{IdT}$					*1*	−0.05	**0.30**	−0.01	**0.30**	−0.03
as BX2*^{2}G36$_{IdT}$						*1*	−0.02	**0.29**	−0.03	**0.29**
s BX2*G2$_{Illum}$							*1*	−0.02	**0.51**	−0.02
as BX2*G2$_{Illum}$								*1*	−0.02	**0.50**
s T-1$_{Illum}$									*1*	*0*
as T-1$_{Illum}$										*1*
			IdT adaptor set					**Illumina adaptor set**		

Using the indicated sets of RNA adapters (*Illum* or *IdT*) to generate small RNA libraries, we had generated 10 sequencing data sets from *BX2* and *T-1* strains under various genetic settings (see text and ref. 14). Sense (s) and antisense (as) piRNA abundance profiles were handled as vectors of 11,690 variables indexed with the *P{lacW}* coordinates and taking as values the number of sequenced piRNAs mapped at these coordinates (most 5' nucleotide location). Pearson (upper table) and Spearman (lower table) correlations between these vectors were then computed in pairwise combinations using the R software. Significant correlations (*P* value < 2.2e−16) are bolded.

the antisense strand of *P{lArB}* (**Fig. 3C**). As mentioned above, we chose the Spearman correlation because it is more stringent when the data do not necessarily come from a bivariate normal distribution. In addition, the 500 nt size of profile segments was a good compromise between the amount of information contained in segments and the number of pairwise correlations to be computed. If higher than 0.3 (*P* value < 2.2e−16), the correlation coefficients were then plotted in a dot matrix. As a result, correlation dot matrixes generated with the sense (**Fig. 3B**) as well as the antisense strand (**Fig. 3C**) of *P{lArB}* echoed the dot matrix of Blastn alignment between *P{lArB}* and *P{lacW}*. Thus, the piRNA abundance profiles generated by both strands of the *lacZ* sequences at the *P-1152* or *T-1* loci strongly correlated with each other. Strikingly, the inverse orientations of the Pbluescript-derived backbones in *P{lArB}* and *P{lacW}* were captured in both correlation dot matrixes (**Fig. 3B and C**), indicating that the profiles of piRNA abundances in the *P-1152* and *T-1* loci are locally determined by DNA sequences but not by their relative orientation.

The extended analysis of our piRNA sequencing data sets suggests that the relative abundance of piRNAs is locally determined in piRNA-producing loci. Further supporting this notion, it was possible to consistently remap transposons and retrotransposons dispersed in the genome by scanning genome-wide piRNA profiles with a sliding window and computing correlations with reference profiles for families of transposons and retrotransposons (data not shown). Several steps in piRNA biogenesis may be sequenced-biased, leading to sequence-dependent profiles of piRNA abundances. Cleavage of long RNA precursors by the Zucchini RNase may involve preferences for local RNA motives and/or local RNA secondary structures. In addition to the established preference of Aubergine and Piwi for piRNAs starting with a 5'U, other sequence motives may be responsible for preferential piRNA loading into these Argonautes. Finally, thermodynamic features and target matches that, in turn, depend on piRNA sequences may influence the stability of piRNAs and, thus, their abundances in small RNA libraries. In any case, our data favor a model in which local sequence rather than long-distance chromosomal environment is a primary determinant of the abundance profiles of piRNAs.

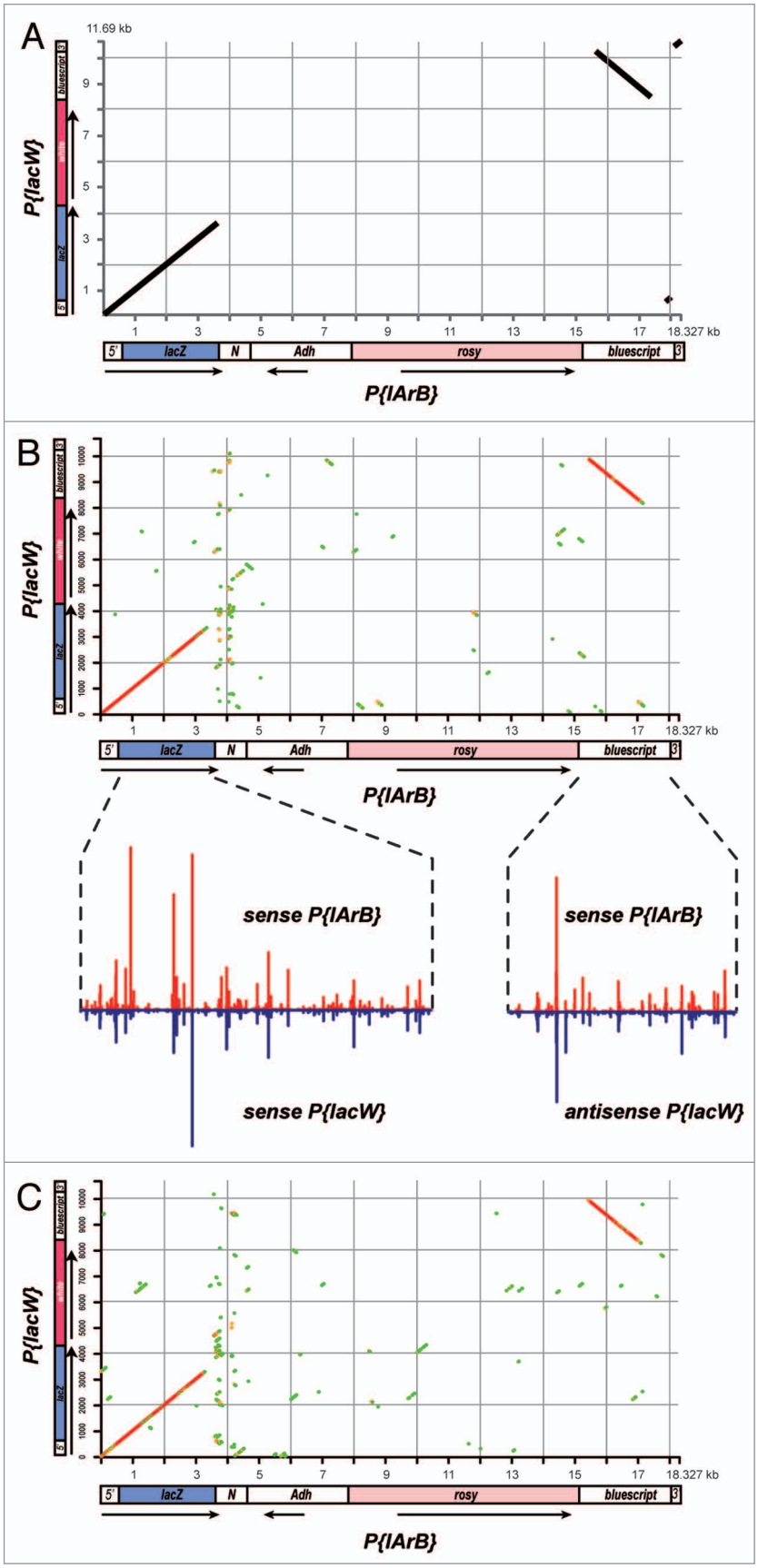

Figure 3. Sequences common to *P{lacW}* and *P{lArB}* in *T-1* and *P-1152* loci, respectively, generate highly similar profiles of piRNA abundances. (**A**) Dot matrix view of a Blastn alignment between *P{lArB}* and *P{lacW}*. In these transgenes, the *lacZ* and *pBluescript* sequences are 100% identical (black lines) and in the same or inverse orientation relatively to the *P*-ends (5' and 3'), respectively. The 620 bp sequence of the region noted N in *P{lArB}* is unknown. (**B**) Spearman correlation matrix between profiles of piRNA abundances from the sense strand of *P{lArB}* and profiles of piRNA abundances from either strands of *P{lacW}*. All possible correlations between 500 nt sliding windows were computed using an in-house python script (available upon request) and the stats.spearman function from the scipy python module. Spearman correlation coefficients were plotted relatively to the 5' coordinates of the windows in *P{lArB}* (x-axis) and *P{lacW}* (y-axis) only if higher than 0.32: in green if lower than 0.35, in orange when between 0.35 and 0.4, and in red if higher than 0.4. For clarity, piRNA profiles from the indicated strands are shown in insets as in **Figure 2** for the *lacZ* and *pBluescript* regions with high profile similarities. The antisense pBluescript profile from *P{lacW}* was reversed before plotting. (**C**) The Spearman correlation matrix between profiles of piRNA abundances from the antisense strand of *P{lArB}* and profiles of piRNA abundances from either strands of *P{lacW}* was computed and displayed as in (**B**).

Disclosure of Potential Conflicts of Interest

No potential conflicts of interest were disclosed.

Acknowledgments

We thank Armand Taranco for helpful discussions on statistical correlations. This work was supported by fellowships from the Ministère de l'Enseignement Supérieur et de la Recherche to AV and CH, from the Fondation pour la Recherche Médicale to AV, from the Association Nationale de la Rercherche (ANR) to ALB, and by grants from the Fondation ARC pour la Recherche contre le Cancer to SR and from the ANR (project "Nuclear endosiRNAs") to CA.

References

1. Guzzardo PM, Muerdter F, Hannon GJ. The piRNA pathway in flies: highlights and future directions. Curr Opin Genet Dev 2013; 23:44-52; PMID:23317515; http://dx.doi.org/10.1016/j.gde.2012.12.003
2. Zhang F, Wang J, Xu J, Zhang Z, Koppetsch BS, Schultz N, et al. UAP56 couples piRNA clusters to the perinuclear transposon silencing machinery. Cell 2012; 151:871-84; PMID:23141543; http://dx.doi.org/10.1016/j.cell.2012.09.040
3. Nishimasu H, Ishizu H, Saito K, Fukuhara S, Kamatani MK, Bonnefond L, et al. Structure and function of Zucchini endoribonuclease in piRNA biogenesis. Nature 2012; 491:284-7; PMID:23064230; http://dx.doi.org/10.1038/nature11509
4. Ipsaro JJ, Haase AD, Knott SR, Joshua-Tor L, Hannon GJ. The structural biochemistry of Zucchini implicates it as a nuclease in piRNA biogenesis. Nature 2012; 491:279-83; PMID:23064227; http://dx.doi.org/10.1038/nature11502
5. Gunawardane LS, Saito K, Nishida KM, Miyoshi K, Kawamura Y, Nagami T, et al. A slicer-mediated mechanism for repeat-associated siRNA 5' end formation in Drosophila. Science 2007; 315:1587-90; PMID:17322028; http://dx.doi.org/10.1126/science.1140494
6. Brennecke J, Aravin AA, Stark A, Dus M, Kellis M, Sachidanandam R, et al. Discrete small RNA-generating loci as master regulators of transposon activity in Drosophila. Cell 2007; 128:1089-103; PMID:17346786; http://dx.doi.org/10.1016/j.cell.2007.01.043
7. Cox DN, Chao A, Lin H. piwi encodes a nucleoplasmic factor whose activity modulates the number and division rate of germline stem cells. Development 2000; 127:503-14; PMID:10631171
8. Saito K, Inagaki S, Mituyama T, Kawamura Y, Ono Y, Sakota E, et al. A regulatory circuit for piwi by the large Maf gene traffic jam in Drosophila. Nature 2009; 461:1296-9; PMID:19812547; http://dx.doi.org/10.1038/nature08501
9. Klenov MS, Sokolova OA, Yakushev EY, Stolyarenko AD, Mikhaleva EA, Lavrov SA, et al. Separation of stem cell maintenance and transposon silencing functions of Piwi protein. Proc Natl Acad Sci USA 2011; 108:18760-5; PMID:22065765; http://dx.doi.org/10.1073/pnas.1106676108
10. Sienski G, Dönertas D, Brennecke J. Transcriptional silencing of transposons by Piwi and maelstrom and its impact on chromatin state and gene expression. Cell 2012; 151:964-80; PMID:23159368; http://dx.doi.org/10.1016/j.cell.2012.10.040
11. Huang XA, Yin H, Sweeney S, Raha D, Snyder M, Lin H. A major epigenetic programming mechanism guided by piRNAs. Dev Cell 2013; 24:502-16; PMID:23434410; http://dx.doi.org/10.1016/j.devcel.2013.01.023
12. Rangan P, Malone CD, Navarro C, Newbold SP, Hayes PS, Sachidanandam R, et al. piRNA production requires heterochromatin formation in Drosophila. Curr Biol 2011; 21:1373-9; PMID:21820311; http://dx.doi.org/10.1016/j.cub.2011.06.057
13. Klattenhoff C, Xi H, Li C, Lee S, Xu J, Khurana JS, et al. The Drosophila HP1 homolog Rhino is required for transposon silencing and piRNA production by dual-strand clusters. Cell 2009; 138:1137-49; PMID:19732946; http://dx.doi.org/10.1016/j.cell.2009.07.014
14. de Vanssay A, Bougé AL, Boivin A, Hermant C, Teysset L, Delmarre V, et al. Paramutation in Drosophila linked to emergence of a piRNA-producing locus. Nature 2012; 490:112-5; PMID:22922650; http://dx.doi.org/10.1038/nature11416
15. Roche SE, Rio DC. Trans-silencing by P elements inserted in subtelomeric heterochromatin involves the Drosophila Polycomb group gene, Enhancer of zeste. Genetics 1998; 149:1839-55; PMID:9691041
16. Josse T, Teysset L, Todeschini AL, Sidor CM, Anxolabéhère D, Ronsseray S. Telomeric trans-silencing: an epigenetic repression combining RNA silencing and heterochromatin formation. PLoS Genet 2007; 3:1633-43; PMID:17941712; http://dx.doi.org/10.1371/journal.pgen.0030158
17. Brennecke J, Malone CD, Aravin AA, Sachidanandam R, Stark A, Hannon GJ. An epigenetic role for maternally inherited piRNAs in transposon silencing. Science 2008; 322:1387-92; PMID:19039138; http://dx.doi.org/10.1126/science.1165171
18. Ronsseray S, Lehmann M, Nouaud D, Anxolabéhère D. The regulatory properties of autonomous subtelomeric P elements are sensitive to a Suppressor of variegation in Drosophila melanogaster. Genetics 1996; 143:1663-74; PMID:8844154
19. Marin L, Lehmann M, Nouaud D, Izaabel H, Anxolabéhère D, Ronsseray S. P-Element repression in Drosophila melanogaster by a naturally occurring defective telomeric P copy. Genetics 2000; 155:1841-54; PMID:10924479
20. Dorer DR, Henikoff S. Transgene repeat arrays interact with distant heterochromatin and cause silencing in cis and trans. Genetics 1997; 147:1181-90; PMID:9383061
21. Ronsseray S, Boivin A, Anxolabéhère D. P-Element repression in Drosophila melanogaster by variegating clusters of P-lacZ-white transgenes. Genetics 2001; 159:1631-42; PMID:11779802
22. Brink RA. A Genetic Change Associated with the R Locus in Maize Which Is Directed and Potentially Reversible. Genetics 1956; 41:872-89; PMID:17247669
23. Coe EH. A Regular and Continuing Conversion-Type Phenomenon at the B Locus in Maize. Proc Natl Acad Sci USA 1959; 45:828-32; PMID:16590451; http://dx.doi.org/10.1073/pnas.45.6.828
24. Grentzinger T, Armenise C, Brun C, Mugat B, Serrano V, Pelisson A, et al. piRNA-mediated transgenerational inheritance of an acquired trait. Genome Res 2012; 22:1877-88; PMID:22555593; http://dx.doi.org/10.1101/gr.136614.111
25. Sorefan K, Pais H, Hall AE, Kozomara A, Griffiths-Jones S, Moulton V, et al. Reducing ligation bias of small RNAs in libraries for next generation sequencing. Silence 2012; 3:4; PMID:22647250; http://dx.doi.org/10.1186/1758-907X-3-4
26. Muerdter F, Olovnikov I, Molaro A, Rozhkov NV, Czech B, Gordon A, et al. Production of artificial piRNAs in flies and mice. RNA 2012; 18:42-52; PMID:22096018; http://dx.doi.org/10.1261/rna.029769.111